GEOPHYSICS, VOL. 51, NO. 2 (FEBRUARY 1986); P. 324–331, 14 FIGS.

Migration of common-shot gathers

Moshe Reshef* and Dan Kosloff*

ABSTRACT

Three depth migration methods which operate on common-shot data are presented. The first migration method maps digitized horizons from the X-T domain to the X-Z domain. Because this method is based on ray tracing, its computation time is short; it is suggested for iterative velocity analysis. The other two migration methods map the entire common-shot gather into a depth section. The common-shot migration requires calculation of the arrival time of the direct wave from the source to all the depth points, and is done through a direct solution of the eikonal equation. All three methods are suitable for areas with both lateral and vertical velocity variation.

INTRODUCTION

It has long been recognized that conventional common-depth-point (CDP) processing is inadequate for areas that are geologically complex. In CDP processing migration is performed at a late stage, after the data have been biased and affected by normal moveout (NMO) correction and CDP stacking. Therefore, time migration (Claerbout and Doherty, 1972; Schneider, 1978; Stolt, 1978) and true depth migration (Judson et al., 1980; Larner et al., 1981; Kosloff and Baysal, 1983) will both operate incorrectly on data collected over areas with large lateral velocity variations and on data with steep dip events.

Some of the stacking effects can be corrected by prestack partial migration, or dip moveout, as suggested by a number of authors (Yilmaz and Claerbout, 1980; Bolondi et al., 1982; Hale, 1984). However, these methods still cannot perform accurately in regions that have complex velocity variations.

Depth migration of common-shot gathers is an alternative to CDP processing and can give correct imaging and better preserve dip and amplitude information. Because a common-shot gather is collected from a single physical experiment, the subsequent data processing can be implemented with fewer restrictions and approximations. In particular, there are no limitations on the velocity variation and the type of geometry that can be used. The need for an accurate migration that will avoid the CDP stacking artifacts is recognized and has induced several authors to suggest methods for prestack migration and common-shot migration (Phinney and Jurdy, 1979; Jain and Wern, 1980; Schultz and Sherwood, 1980).

This study presents three methods for migrating common-shot data.

The first method is a ray-tracing technique which maps digitized events from the time section into a depth section. This migration is analogous to methods introduced for migration of stacked sections (May and Covey, 1981), except this migration satisfies the imaging condition that requires a ray-tracing calculation from both the source location and the receiver position.

The second method is a full wave-equation migration similar to the poststack depth migration in Kosloff and Baysal (1983), except for a different imaging condition. Instead of using the amplitude values at time zero, as in poststack migration, the depth section now consists of the amplitudes at the time of arrival of the direct wave from the source. The direct arrival time is calculated through direct solution of the eikonal equation.

The third method uses source and receiver pairs. For each pair, the eikonal equation is solved twice: once for the source, then for the receiver. The output depth section consists of the sum of contributions of all the pairs. Since the source is common to all the receivers, the method requires solving the eikonal equation for the source position and each of the receiver locations. The following sections describe the three migration methods. Also presented are synthetic examples which demonstrate important features of the methods.

RAY-TRACING MIGRATION

In this method selected horizons are digitized from the shot gather, and projected downward by ray tracing. The following derivation is for an isovelocity layered structure, although the method can be generalized to a continuously varying velocity field in each layer. The angle of emergence of each ray at a given receiver is determined from the ray parameter, calculated from the traveltime curve. As described in Figure 1, the selected traveltime curve was digitized and a cubic spline passing through the digitized points was calculated. The ray parameter (dT/dx in Figure 1) was determined from the deriva-

Manuscript received by the Editor February 14, 1985; revised manuscript received July 30, 1985.
*Department of Geophysics and Planetary Sciences, Tel Aviv University, Tel Aviv 69978, Israel.
© 1986 Society of Exploration Geophysicists. All rights reserved.

Downloaded 06 Jun 2012 to 72.20.129.98. Redistribution subject to SEG license or copyright; see Terms of Use at http://segdl.org/

tives of the splines at each receiver position $X = R$. Each source-receiver pair contributes one depth point for each projected horizon. The assembly of these points defines the reflector. Calculation of a depth point on the first horizon is shown in Figure 2. Knowing the velocity (V_1), the angle δ, and the two-way traveltime (t_1) detected at **R**, the slope β can be determined by simple trigonometry. The slope δ was calculated from the ray parameter. The depth point O(x, z) is the intersection between the lines OR and OS. The reflector slope at this point is perpendicular to the bisector of the angle 2ν.

After the first horizon is determined, the migration proceeds to the next reflector. As shown in Figure 3, ray tracing is started from the receiver (**R**) with the angle of emergence δ which was calculated from $(dT/dx)_2$ (see Figure 1). Knowing the velocity V_2, we can cross the first reflector at point O and send an infinite ray (linear line) into the lower half-space. To find the second reflector's point F, a search is performed among different rays from the source location (two of these paths are marked 1 and 2 in Figure 3). Point F is the point which satisfies the imaging condition

$$\frac{SP}{V_1} + \frac{PF}{V_2} + \frac{FO}{V_2} + \frac{OR}{V_1} = t_2, \qquad (1)$$

where t_2 is the two-way traveltime measured at receiver **R**.

Figure 4 shows some raypaths for a shot and a set of receivers over a three-layered model with velocities of 2 000, 2 500, and 3 000 m/s, respectively. A synthetic time section was calculated for a set of 90 receivers with spacing of 30 m. The time increment was 0.001 s (Figure 5). Results of the ray-tracing migration along with the input depth horizons are shown in Figure 6. As expected, the area of coverage narrows with depth and the density of the reconstructed depth points is not uniform (compare with the raypaths in Figure 4). To overcome the coverage problem, we can construct the first horizon from a large set of partially overlapping common-shot gathers, continue to the second horizon for all the shots, and then continue for all the remaining horizons. The density of the reconstructed depth points will depend upon the amount of overlap between the processed shot gathers.

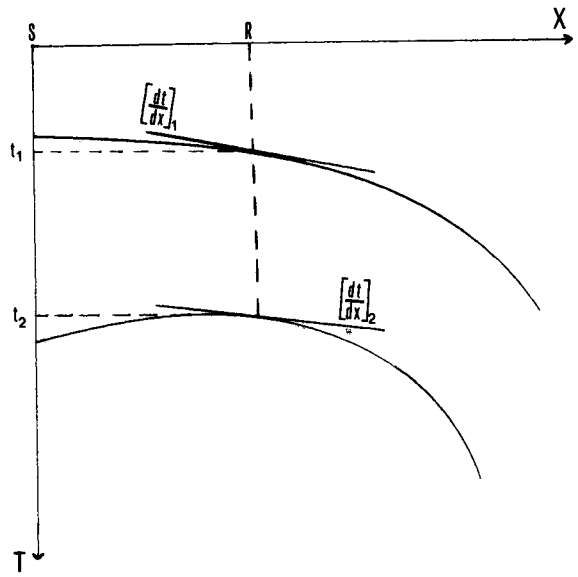

FIG. 1. Determination of the ray parameter.

The method presented involves only simple ray-tracing calculations and is therefore relatively fast. Consequently, one important application is an iterative determination of the interval velocities. Such an implementation is given in the following two examples. The first example, shown in Figure 7, presents results of migrating a horizon with an error of ± 10 percent in interval velocity values (some raypaths are given for reference). It is assumed in this example that the velocity is known for shot 1 (S_1); a velocity determination for shot 2 (S_2) is required. As seen in the example, the error in velocity determination will occur as a sharp discontinuity in the reflector. Using the correct velocity will result in a continuous reflector.

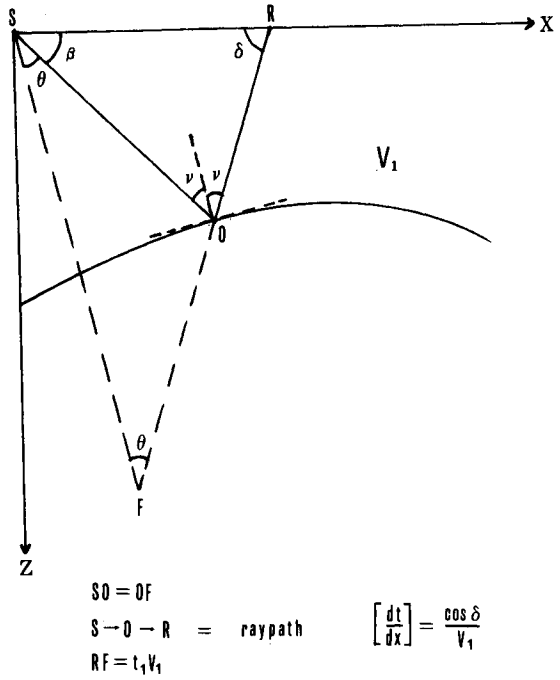

FIG. 2. Determination of a depth point on the first reflector.

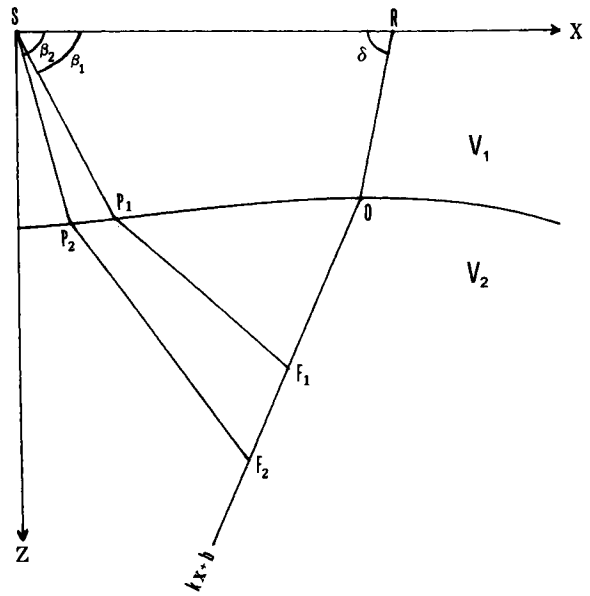

FIG. 3. Determination of a depth point on the second reflector.

Downloaded 06 Jun 2012 to 72.20.129.98. Redistribution subject to SEG license or copyright; see Terms of Use at http://segdl.org/

When there is no knowledge of the velocity, two opposite sides of two partially overlapped spreads (Figure 8a) can be used. Results of migrating the horizon with different interval velocity values are shown in Figure 8b. It is evident that a continuous reflector will result only when mapping both gathers into depth with the correct velocity.

WAVE-EQUATION MIGRATION

Wave-equation migration is based on downward continuation of the acoustic wave equation, where the downward continuation process is almost identical to that used for depth migration of stacked sections (Kosloff and Baysal, 1983). The main difference is in the imaging condition. Assuming that a reflector exists whenever the direct wave from the source and the reflected wave are time-coincident (Claerbout, 1976), the depth section will consist of the wave amplitudes at the given depth location at the time of the arrival of the direct wave. Let $P(x, Z = 0, t)$ denote the recorded common-shot gather at the Earth's surface. The final section will then consist of $P(X, Z, t_d)$, where t_d is the arrival time of the direct wave from the source to the depth points (X, Z). When the calculation is in

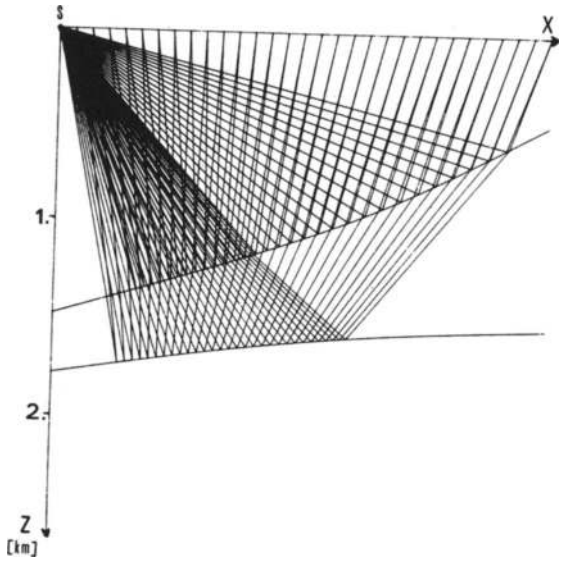

FIG. 4. Raypaths geometry for the three-layered model. Velocities are 2 000, 2 500, and 3 000 m/s for the upper, middle, and lower regions, respectively.

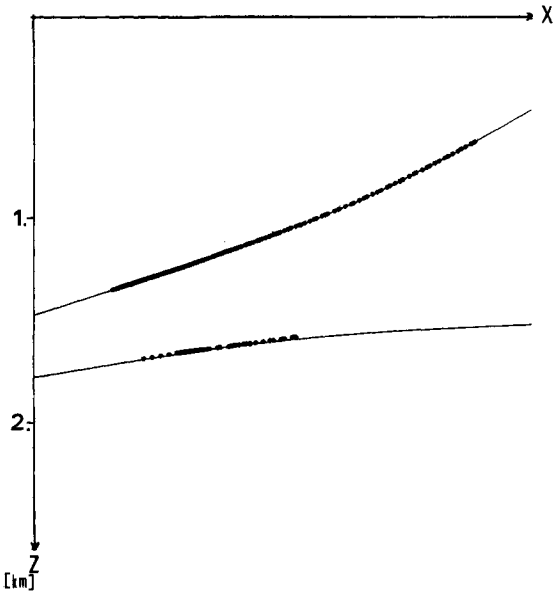

FIG. 6. Ray-tracing migration, results for the three-layered model (solid lines indicate the initial layers).

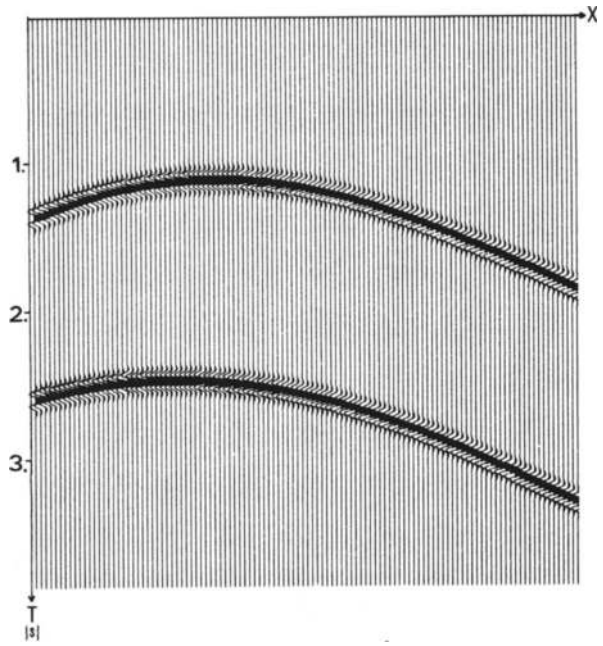

FIG. 5. Synthetic time section for the three-layered model.

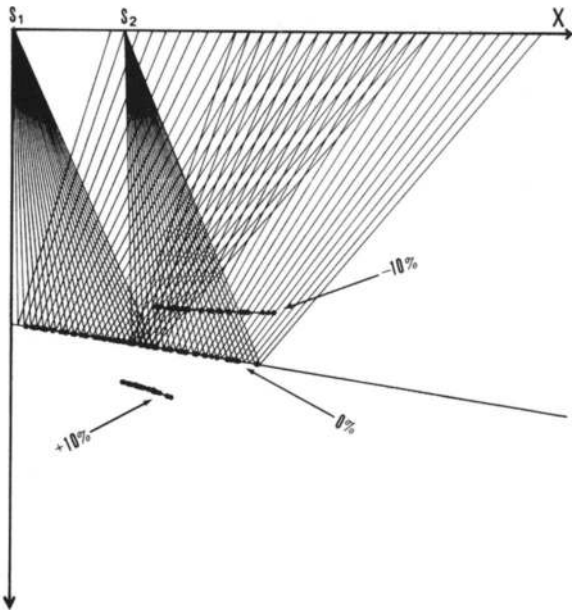

FIG. 7. Velocity analysis technique, the velocity model for the first shot is known.

Downloaded 06 Jun 2012 to 72.20.129.98. Redistribution subject to SEG license or copyright; see Terms of Use at http://segdl.org/

the space-frequency domain, the final depth section is given by

$$\tilde{P}(X, Z, t_d) = \sum_{\omega} \tilde{P}(X, Z, \omega) e^{i\omega t_d}, \quad (2)$$

where the summation is over the seismic frequency band. For migration based on primary arrivals only, a version of the nonreflecting wave equation introduced in Baysal et al. (1984) is most suitable for downward continuation. The basic equation for depth stepping is

$$\frac{\partial}{\partial Z}\begin{bmatrix} \tilde{P} \\ C\dfrac{\partial \tilde{P}}{\partial Z} \end{bmatrix} = \begin{bmatrix} 0 & \dfrac{1}{C} \\ C\left(\dfrac{-\omega^2}{C^2} - \dfrac{\partial^2}{\partial X^2}\right) & 0 \end{bmatrix} \begin{bmatrix} \tilde{P} \\ C\dfrac{\partial \tilde{P}}{\partial Z} \end{bmatrix}, \quad (3)$$

where X, Z are Cartesian coordinates, ω is the frequency, $C(X, Z)$ is the acoustic velocity, and $\tilde{P}(X, Z, \omega)$ is the transformed pressure field. Equation (3) is different from the equation presented by Baysal et al. (1984) in that it is a nonreflecting equation only in the Z direction.

The solution of this equation is obtained through standard integration techniques for solving ordinary differential equations. We adopted a highly accurate, efficient method developed in Tal-Ezer (1984). A brief description and implementation of the method to the solution of equation (3) is given in the Appendix.

The input for common-shot migration consists of the pressure field on the Earth's surface, $P(X, Z = 0, t)$; the acoustic velocity, $C(X, Z)$; and the direct arrival time, $t_d(X, Z)$. In addition, values of $\partial P/\partial Z(X, Z = 0, t)$ on the earth's surface need to be generated as in Kosloff and Baysal (1983). The output yields the depth section $P(X, Z, t_d)$. Figure 9 shows results of the migration after using the input time section shown in Figure 5 with the velocity model shown in Figure 4. Figure 9 shows that the migration was able to map all events to their correct positions.

For wave amplitudes, the use of the eikonal equation precludes completely accurate values. Possibly, the values of the reflection coefficients of interfaces can be extracted by using other methods for the direct arrivals (Temme, 1984), but this point is beyond the scope of this work. Since common-shot migration is based on single physical experiments, we expect more amplitude information to be presented than is CDP stacking.

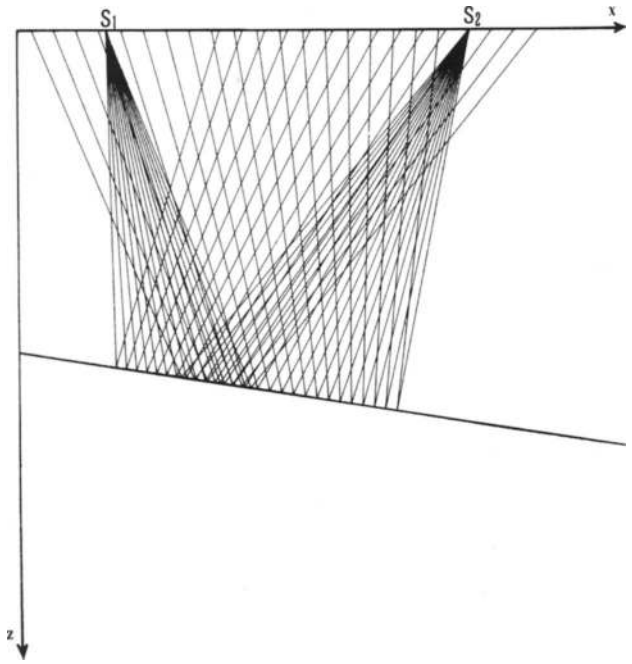

FIG. 8a. Raypaths of two partially overlapped shot gathers.

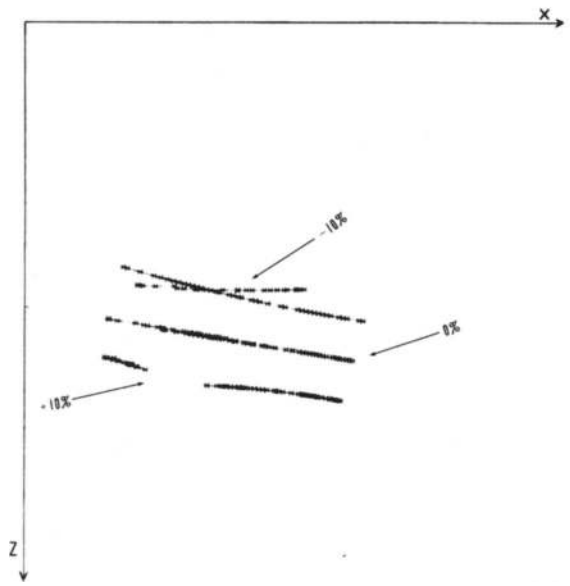

FIG. 8b. Velocity analysis technique, unknown velocities.

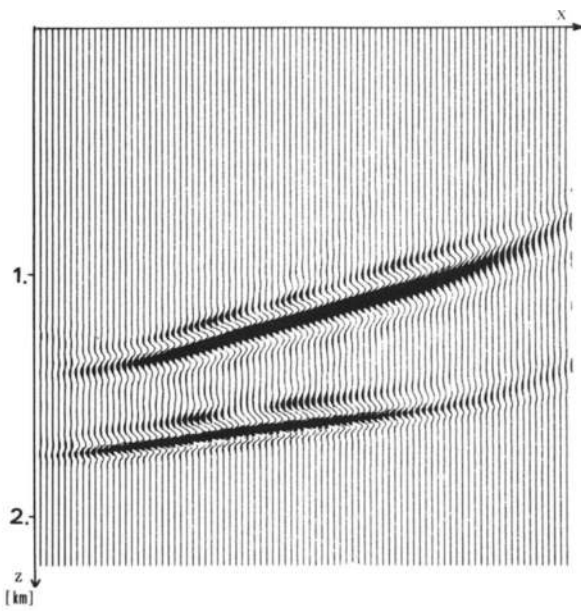

FIG. 9. Wave-equation migration, results for the three-layered model.

Downloaded 06 Jun 2012 to 72.20.129.98. Redistribution subject to SEG license or copyright; see Terms of Use at http://segdl.org/

CALCULATION OF THE DIRECT WAVE ARRIVAL TIME

As mentioned, the common-shot migration requires the function $t_d(X, Z)$, the arrival time of the direct wave from the source, as an input. Therefore a special calculation is needed to determine this function. In principle, t_d can be calculated by ray tracing from the source to all depth points in the numerical mesh. However this ray tracing can be time-consuming; hence we chose to calculate t_d by direct solution of the eikonal equation.

In a two-dimensional acoustic medium, the eikonal equation is

$$\left(\frac{\partial T}{\partial X}\right)^2 + \left(\frac{\partial T}{\partial Z}\right)^2 = \frac{1}{C^2}, \tag{4}$$

where T is the traveltime and $C(X, Z)$ is the acoustic velocity (e.g., Stavrodis, 1972).

For numerical integration we write the equation explicitly as

$$\frac{\partial T}{\partial Z} = \left[\frac{1}{C^2} - \left(\frac{\partial T}{\partial X}\right)^2\right]^{1/2} \tag{5}$$

In the solution scheme, $\partial T(X, Z)/\partial X$ is calculated by a finite-difference approximation based on the values $T(X, Z)$ at the given horizon Z. Stepping in depth is carried out by a fourth-order Runga-Kutta method. For initialization of the solution values, the values of $T(X, Z = 0)$ at the surface need to be specified; they can be calculated directly in the case of a uniform surface velocity or otherwise by ray tracing. During the integration careful attention must be given to the possibility of discontinuous time fronts, as in the case of postcritical angles on an interface. Two examples of the eikonal solution are shown in Figures 10a and 10b. The source is at the upper right corner and time contours as a function of X-Z are shown for an increasing velocity model (Figure 10a) and a low-velocity region model (Figure 10b). The traveltime function for the discontinuity points along the low-to-high velocity boundaries was calculated by ray tracing. These values can replace the values that were obtained by the Runge-Kutta method. Notice that the integration scheme eliminates the upgoing waves from the solution, so in the case of a strongly inhomogeneous medium, generalized ray-tracing methods should be used.

TWO-EIKONAL METHOD

The ability to solve the eikonal equation raises the possibility of a common-shot migration based exclusively on the eikonal equation. In this method, the final depth section is progressively calculated from contributions from shot-receiver pairs, requiring solution of the eikonal equation with source positions at the shot location and also at all receiver locations.

For illustration, we consider migration of a synthetic example containing one event corresponding to a reflection in a uniform velocity medium. We first consider the contribution from one source-receiver pair. For a given depth point (X, Z), a reflection event from the source S to the receiver R occurs only at a time t^*. This time is equal to the time t_d for a wave to propagate from the source to the given point (X, Z), plus the time t_r for the reflected wave to propagate from the point to the receiver. Consequently, the contribution to the amplitude at the point (X, Z) from the source-receiver pair will be equal to the amplitude of the receiver trace at time $t^* = t_d + t_r$ (Figure 11). The amplitude of the final section at the point $(X,$

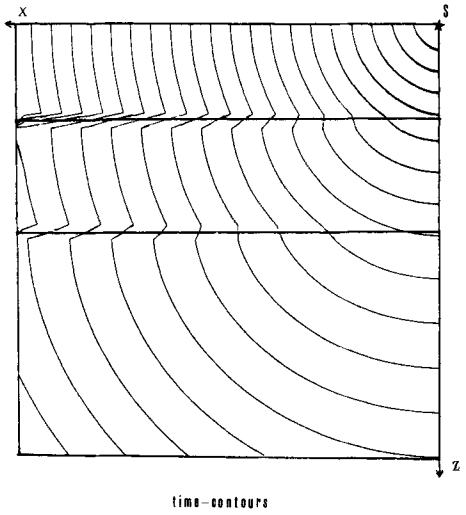

FIG. 10a. Eikonal equation solution for the increasing velocity model.

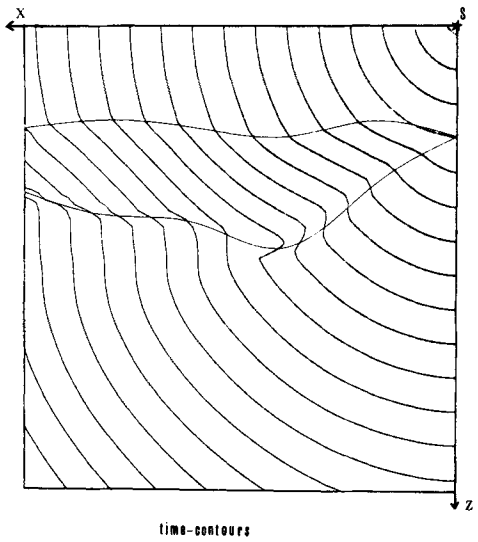

FIG. 10b. Eikonal equation solution for the low-velocity region model.

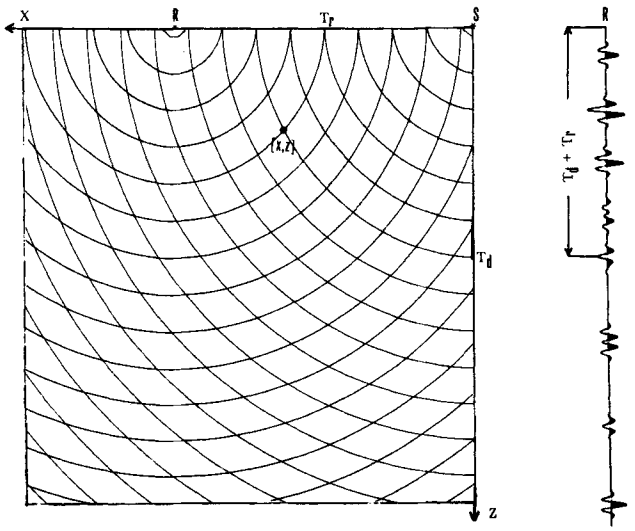

FIG. 11. Contribution from a source-receiver pair to a depth point.

Downloaded 06 Jun 2012 to 72.20.129.98. Redistribution subject to SEG license or copyright; see Terms of Use at http://segdl.org/

Z) will be the sum of the contributions from all shot-receiver pairs. The values of $t_d(X, Z)$ and $t_r(X, Z)$ are obtained by solving the eikonal equation for the shot and the receiver positions, respectively.

For the example with a single layer, the resulting trace at the receiver R will contain a single event at time t^*. For the source-receiver pair, the locus of all points for which $t_d(X, Z) + t_r(X, Z) = t^*$ defines one ellipse in depth. The actual depth position of the layer is given by the envelope of all ellipses obtained from shot-receiver pairs. For the upper event shown in Figure 5, consecutive construction of the final section, first with one shot-receiver pair and then with two (4 and 90 pairs, respectively) is shown in Figures 12a–12d. So far, construction of a depth section from a single shot gather has been considered. However, it can be expected that stacking of final depth sections from several shot gathers can bring about signal-to-noise enhancements similar to those obtained in CDP stacking. For demonstration, the model shown in Figure 4 is reconsidered. Synthetic time sections were calculated for different shot locations with random noise added (one of the shot gathers is shown in Figure 13). The two-eikonal method was used for the migration. Results of the migration for depth stacking, with shots at every eight receiver positions and every fourth receiver position, are shown in Figure 14a and 14b, respectively. The reflectors, as the figures show, are well reconstructed even in the example where every eighth shot gather is stacked. Noise is almost entirely eliminated by stacking when the shots are at every fourth receiver location.

CONCLUSIONS

We presented three methods for common-shot migration, all designed for migration of data from regions with severe vertical and lateral velocity variation. Extensive testing of the

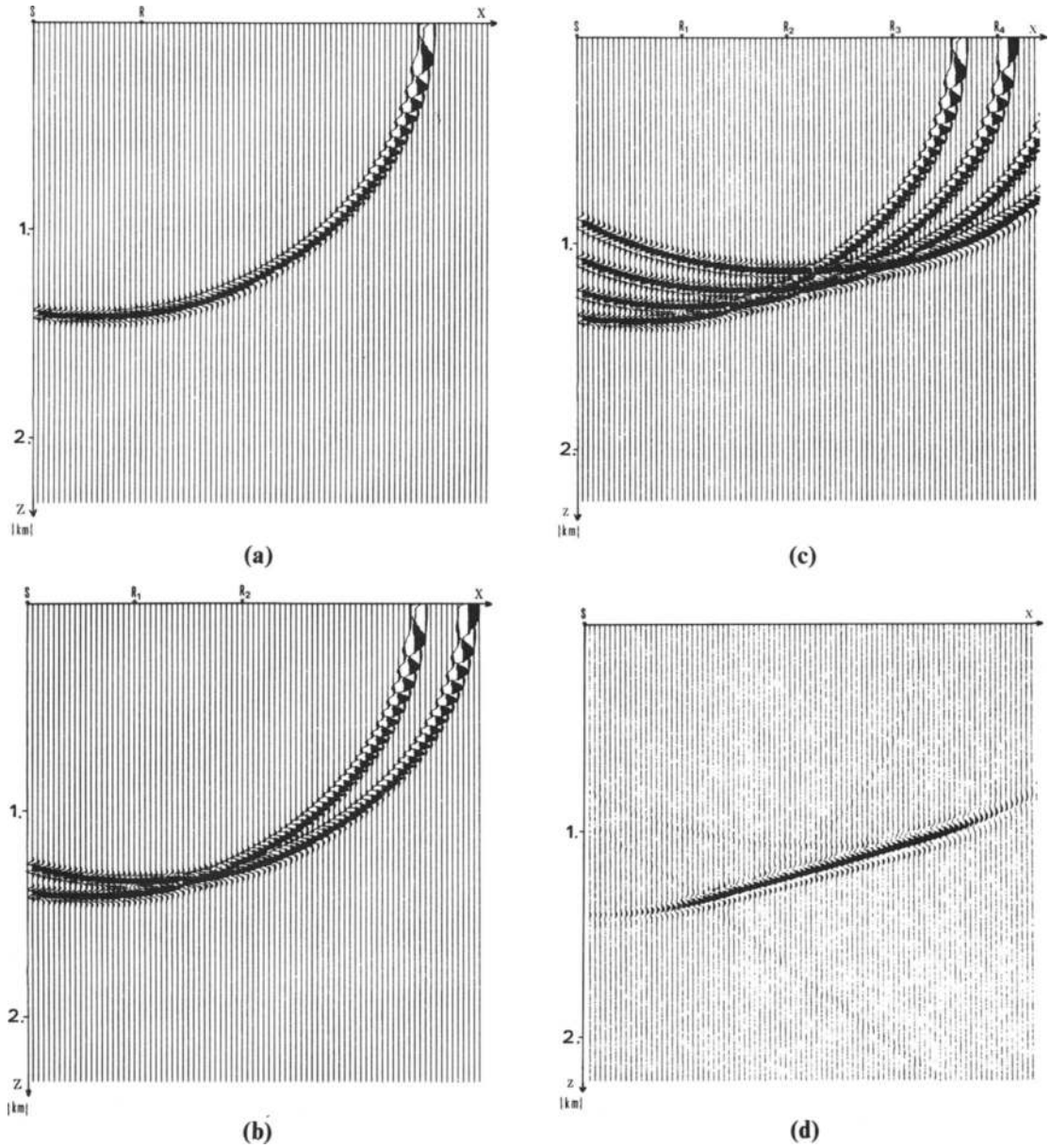

FIG. 12. (a) Depth section for a single-layer model, contribution from one source-receiver pair. (b) Depth section for a single-layer model, contribution from two source-receiver pairs. (c) Depth section for a single-layer model, contribution from four source-receiver pairs. (d) Depth section for a single-layer model, contribution from 90 source-receiver pairs.

Downloaded 06 Jun 2012 to 72.20.129.98. Redistribution subject to SEG license or copyright; see Terms of Use at http://segdl.org/

methods on different types of field data is required to evaluate their effectiveness. Implementation of methods with field data will require an effective technique for velocity analysis. This study suggests use of ray-tracing migration for an iterative velocity analysis. However, such migration requires identification of events on the shot gather, a task which is not always possible. Additional velocity determination techniques are therefore required.

Signal-to-noise improvement may be achieved by stacking of depth-migrated common-shot gathers. The optimal amount of overlap needs to be determined from practical experience. The attractive feature of this type of stacking is that it is done late in the data processing. Thus, this stacking will not bias results against steeply dipping events, as CDP processing often does.

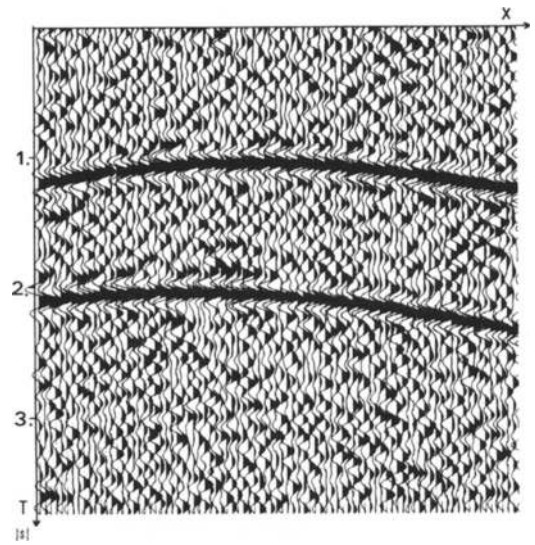

FIG. 13. Synthetic time section for the three-layered model with random noise added.

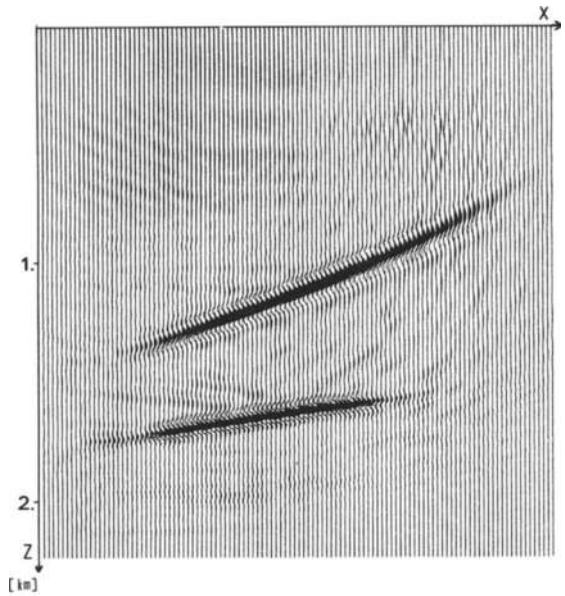

(a)

FIG. 14a. Two-eikonal method, result from depth stacking with shot located at every eighth receiver position.

Comparing the two migration methods that operate on the entire time section, it appears that wave-equation migration will preserve amplitude values better, while the two-eikonal migration is preferable for data collected with unequally spaced receivers. This feature may gain added importance when the migration methods are extended to three dimensions.

REFERENCES

Baysal, E., Kosloff, D., and Sherwood, J. W. C., 1984, A two-way nonreflecting wave equation: Geophysics, **49**, 132–141.
Bolondi, G., Loinger, E., and Rocca, F., 1982, Offset continuation of seismic sections: Geophys. Prosp., **30**, 813–828.
Claerbout, J. F., and Doherty, S. M., 1972, Downward continuation of moveout corrected seismograms: Geophysics, **37**, 741–768.
Claerbout, J. F., 1976, Fundamentals of geophysical data processing: McGraw-Hill Book Co.
Hale, D., 1984, Dip moveout by Fourier transform: Geophysics, **49**, 741–759.
Jain, S., and Wren, A. E., 1980, Migration before stack—Procedure and significance: Geophysics, **45**, 204–212.
Judson, D. R., Lin, J., Schultz, P. S., and Sherwood, J. W. C., 1980, Depth migration after stack: Geophysics, **45**, 361–375.
Kosloff, D., and Baysal, E., 1983, Migration with the full wave equation: Geophysics, **48**, 677–687.
Kosloff, D., Kessler, D., and Koren, Z., 1985, Generalized phase shift migration of stacked section: preprint.
Larner, K. L., Hatton, L., and Gibson, B. S., 1981, Depth migration of imaged time sections: Geophysics, **46**, 734–750.
May, B. T., and Covey, J. D., 1981, An increase ray method for computing geologic structures from seismic reflections—Zero-offset case: Geophysics, **46**, 268–287.
Phinney, R. A., and Jurdy, D. M., 1979, Seismic imaging of deep crust: Geophysics, **44**, 1637–1666.
Schneider, W., 1978, Integral formulation for migration in two and three dimensions: Geophysics, **43**, 49–76.
Schultz, P., S., and Sherwood, J. W. C., 1980, Depth migration before stack: Geophysics, **45**, 376–393.
Stavrodis, O. N., 1972, The optics of rays, wavefronts and caustics: Academic Press, Inc.
Stolt, R. H., 1978, Migration by Fourier transform: Geophysics, **43**, 23–48.
Tal-Ezer, H., 1984, Spectral methods in time for hyperbolic equations: ICASE rep. 172302, NASA Langly Research Center.
Temme, P., 1984, A comparison of CMP single shot and plane wave depth migration: Geophysics, **49**, 1896–1907.
Yilmaz, O., and Claerbout, J. F., 1980, Prestack partial migration: Geophysics, **45**, 1753–1779.

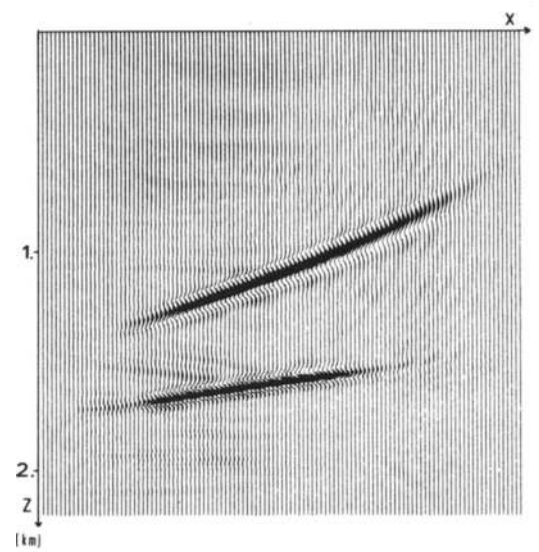

(b)

FIG. 14b. Two-eikonal method, result after depth stacking with shot located at every fourth receiver position.

Downloaded 06 Jun 2012 to 72.20.129.98. Redistribution subject to SEG license or copyright; see Terms of Use at http://segdl.org/

APPENDIX

SOLUTION METHOD FOR WAVE-EQUATION MIGRATION

In this appendix we briefly outline the integration method used for solving equation (3). A more complete discussion of this method was given in Tal Ezer (1984) and Kosloff et al. (1985).

The basic system to be solved in depth is

$$\frac{\partial}{\partial Z}\begin{bmatrix}\tilde{P}\\ C\dfrac{\partial \tilde{P}}{\partial Z}\end{bmatrix}=\begin{bmatrix}0 & \dfrac{1}{C}\\ C\left(\dfrac{-\omega^2}{C^2}-\dfrac{\partial^2}{\partial X^2}\right) & 0\end{bmatrix}\begin{bmatrix}\tilde{P}\\ C\dfrac{\partial \tilde{P}}{\partial Z}\end{bmatrix},$$

where X, Z are Cartesian coordinates, ω is the frequency $C(X, Z)$ is the acoustic velocity, and $\tilde{P}(X, Z, \omega)$ is the transformed pressure field. After spatial discretization in the horizontal direction, equation (3) becomes a set of $2N_x$ coupled ordinary differential equations with the unknown $(\tilde{P})_j(\partial\tilde{P}^2/\partial Z)_j$, $j = 1, \ldots, N_x$, where N_x denotes the number of seismic traces.

The system to be solved is therefore of the form

$$\frac{\partial \mathbf{V}}{\partial Z} = (B)\mathbf{V}, \tag{A-1}$$

where $\mathbf{V}$ is the vector of length $2N_x$ of $\tilde{P}$ and $(C)(\partial\tilde{P}/\partial Z)$, and B is the discretized version of

$$\begin{bmatrix}0 & \dfrac{1}{C}\\ C\left(\dfrac{-\omega^2}{C^2}-\dfrac{\partial^2}{\partial X^2}\right) & 0\end{bmatrix}$$

after elimination of evanescent energy (Kosloff and Baysal, 1983). The evaluation of B in this study was carried out by the Fourier method as in Kosloff and Baysal (1983).

The numerical solution of equation (A-1) is carried out in depth levels. The formal solution at depth $Z + DZ$ is calculated from the solution at depth Z by

$$\mathbf{V}_{Z+DZ} = e^{BDZ}\mathbf{V}_Z, \tag{A-2}$$

where e^{BDZ} is the exponential operator (Tal Ezer, 1984). This relation is evaluated by a Chebychev expansion according to

$$\mathbf{V}_{Z+DZ} = e^{BDZ}\mathbf{V}_Z = \sum_{K=0}^{m} \alpha_K J_K(R) Q_K\left(\frac{\Delta Z}{R}\cdot B\right)\mathbf{V}_Z, \tag{A-3}$$

with $\alpha_0 = 1$ and $\alpha_K = 2$ for $K > 1$. The Kth order Bessel function is denoted by $J_K(R)$. For the migration, $R = \alpha_0/C_{\min}$, with $C_{\min}$ denoting the lowest velocity at depth Z. Chebychev polynomials of the operator $\Delta Z/R \cdot B$ are denoted by Q_K, and are generated recursively according to

$$Q_0\left(\frac{\Delta Z}{R}B\right)V_Z = V_Z, \tag{A-4}$$

$$Q_1\left(\frac{\Delta Z}{R}\cdot B\right)V_Z = \frac{\Delta Z}{R}BV_Z, \tag{A-5}$$

and

$$Q_K\left(\frac{\Delta Z}{R}B\right)V_Z = \left[2\frac{\Delta Z}{R}BQ_{K-1}\left(\frac{\Delta Z}{R}B\right) + Q_{K-2}\left(\frac{\Delta Z}{R}B\right)\right]V_Z \tag{A-6}$$

(Tal Ezer, 1984). The value m at which the expansion (A-3) is truncated is determined when the value of $J_K(R)$ becomes sufficiently small (Kosloff et al., 1985).

Downloaded 06 Jun 2012 to 72.20.129.98. Redistribution subject to SEG license or copyright; see Terms of Use at http://segdl.org/